

## §1. Transport Code Development for ITB Formation and Impurity Control

Yamazaki, K., Oishi, T., Arimoto, H. (Nagoya Univ.), Funaba, H.

The operation with Internal Transport Barrier (ITB) is expected as a high performance operation. ITB is utilized to improve core plasma confinement in the reversed magnetic shear. It is considered that the changes of core plasma profile by the ITB cause changes of impurity transport. In a large fusion reactor, high-Z materials will be used as plasma facing components because high loads of heat and particles concentrate there. However, high-Z impurities from these components cause large radiation loss and dilute the fuel even if the amount of impurities is small. Therefore, in this study, firstly, the ITB formation which includes the effects of the magnetic shear and perturbed profiles by the pellet injection was simulated using the Toroidal Transport Analysis Linkage code TOTAL. Secondly, we analyzed transport of the tungsten impurities using an impurity model in TOTAL code, and compared the impurity profile in the case with ITB to the one without ITB in the tokamak reactor. The impurities decreased in the ITB formation region when ITB was formed, and the outward flux of total impurity density was observed there. It can be expected that outward flux of impurities is generated by the temperature and the density gradients.

The transport simulations<sup>1)</sup> have been carried out focusing on the ITB formation in tokamak and helical plasmas. The ITB model based on Bohm and Gyro Bohm-like transport with  $E \times B$  shear flow effects has already been compared with the JET experimental ITB in tokamak systems and in helical system compared with LHD. This model is introduced into the toroidal transport linkage TOTAL code, and is applied to the 1-dimensional (1-D) ITB formation simulation of 2-D equilibrium for tokamak plasmas and 3-D equilibrium for helical plasmas.

Typical simulation results on ITER plasma with tungsten impurities are shown here. Figure 1 shows the time evolution of the fusion power, heating power and average electron temperature in this operation. Impurities were added at 100 s in the stationary state. Then, the outputs decrease temporarily, and they become stationary state again. This stationary state is discussed in this section.

Figure 2 shows the radial profiles of the core plasma and tungsten impurity density at the 160 s in Fig. 1. The core plasma profiles (electron density, temperature and thermal diffusion coefficient) are shown in (a) and (b), the tungsten density profiles of each ion and their summation denoted as “total” in this figures are shown in (c) and (d). Left figures: (a) and (c) are the cases of operation without ITB, and right figures are the cases with ITB. In the present model, the ITB formation is determined roughly by  $\omega_{E \times B} > \gamma_{ITG}$ . The time-evolution of the criterion parameter depends

on magnetic shear and local density gradient induced by the pellet injection. Here we assumed typical core transport coefficient without or with ITB to clarify impurity ion dynamics.

The change of impurity transport was observed in the presence of ITB, and the decrease of impurities could be confirmed in the ITB formation region. However, the significant change did not appear in the impurity density accumulated in the center. In the case that ITB is formed, it can be expected that outward flux of impurities is generated by the temperature and the density gradient.

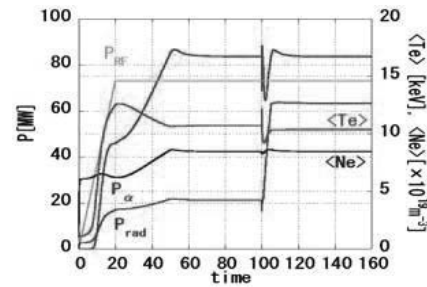


Fig. 1 ITER plasma simulation with impurities added at 100 s, showing time-evolutions of alpha heating power  $P_{\alpha}$ , external heating power  $P_{RF}$ , radiation power  $P_{rad}$ , average electron temperature  $\langle T_e \rangle$  and average electron density  $\langle N_e \rangle$ .

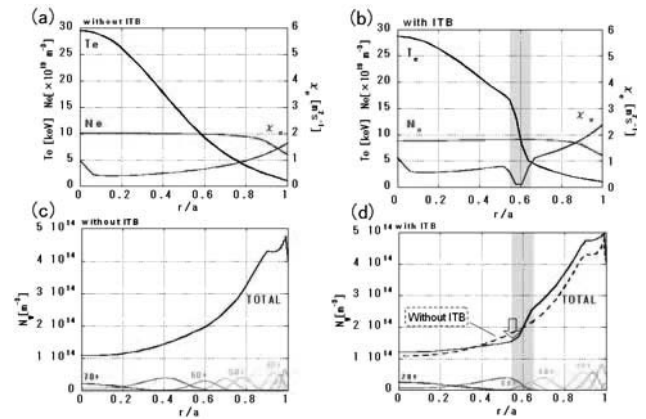


Fig.2 Radial profiles at 160 s. Upper figures show electron density  $N_e$ , temperature  $T_e$  and thermal diffusion coefficient  $\chi_e$  profiles. Lower figures show the tungsten density profiles of each ion and their summation (denoted as “total” in this figures). Left figures show without ITB formation cases. Right figures are with ITB formation cases.

1) Y. Hori, K. Yamazaki, T. Oishi, H. Arimoto and T. Shoji, Plasma and Fusion Research 6 (2011) 2403140.